Science Advances
AAAS

advances.sciencemag.org/cgi/content/full/5/3/eaav9788/DC1

Supplementary Materials for

Immunomodulatory nanogels overcome restricted immunity in a murine model of gut microbiome–mediated metabolic syndrome

Matthew J. Mosquera, Sungwoong Kim, Hao Zhou, Tina T. Jing, Marysol Luna, Jason D. Guss, Pooja Reddy, Kristine Lai, Cynthia A. Leifer, Ilana L. Brito, Christopher J. Hernandez, Ankur Singh*

*Corresponding author. Email: as2833@cornell.edu

Published 27 March 2019, *Sci. Adv.* **5**, eaav9788 (2019)
DOI: 10.1126/sciadv.aav9788

This PDF file includes:

Supplementary Figures

A

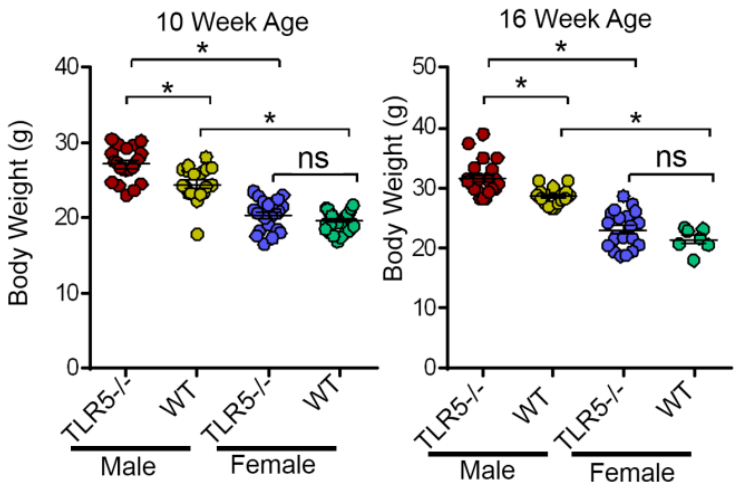

B

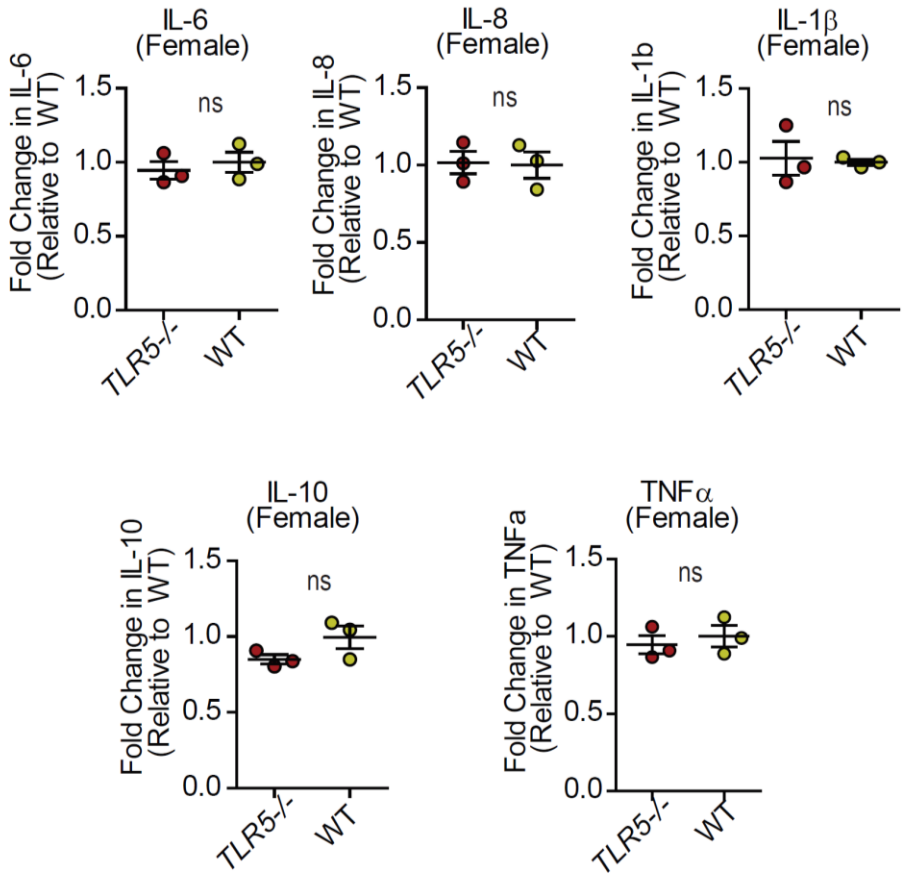

Fig. S1. Characterization of WT and TLR5$^{-/-}$ mice (related to Fig. 1). A) Male and female WT and *TLR5-/-* mice were compared for weight change at 10 and 16 weeks age, as well as a function of gender. Results are presented as Mean ± SEM. Statistics was performed using 1-way ANOVA with Tukey's multiple comparison test. (N=21 *TLR5-/-* Male, N=20 WT Male, N=22 *TLR5-/-* Female, N=31 WT Female). B) Comparison of inflammatory markers in *TLR5-/-* versus WT female mice. Statistics was performed using an unpaired, two-tailed t-test (N=3). (* denotes $p<0.05$, ns denotes non-significant differences between groups.)

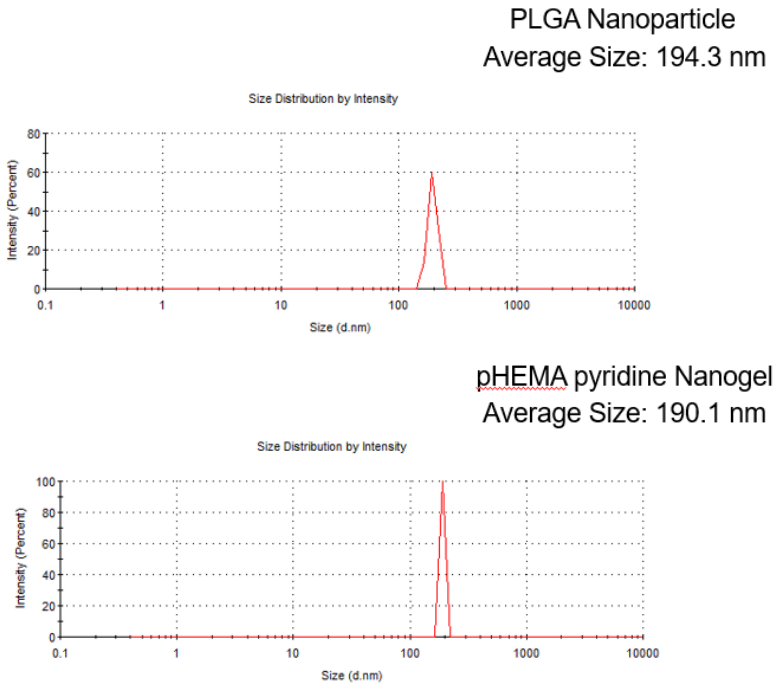

Fig. S2. Pyr-pHEMA nanogels are equivalent in size to PLGA nanoparticle vaccines (related to Fig. 1 and Fig. 5). Pyr-pHEMA nanogel size was compared to a PLGA nanoparticle using a dynamic light scattering instrument.

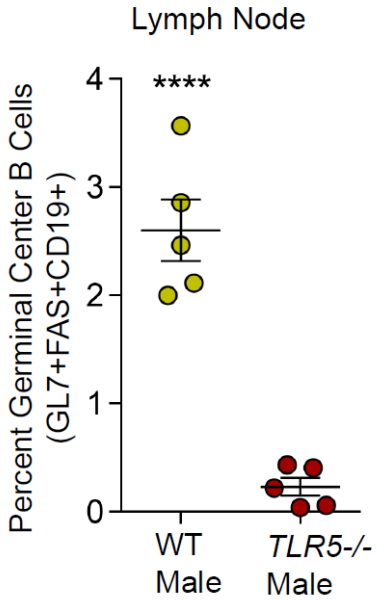

Fig. S3. Knockout of the TLR5 receptor results in lower germinal center formation in mice immunized with a PLGA nanovaccine (related to Fig. 1). Percent CD19+GL7+CD95+ B cells in lymph node cells from immunized mice, six days after booster immunization. Groups were compared with an unpaired, two tailed t-test. (N=5) (**** denotes $p < 0.0001$.)

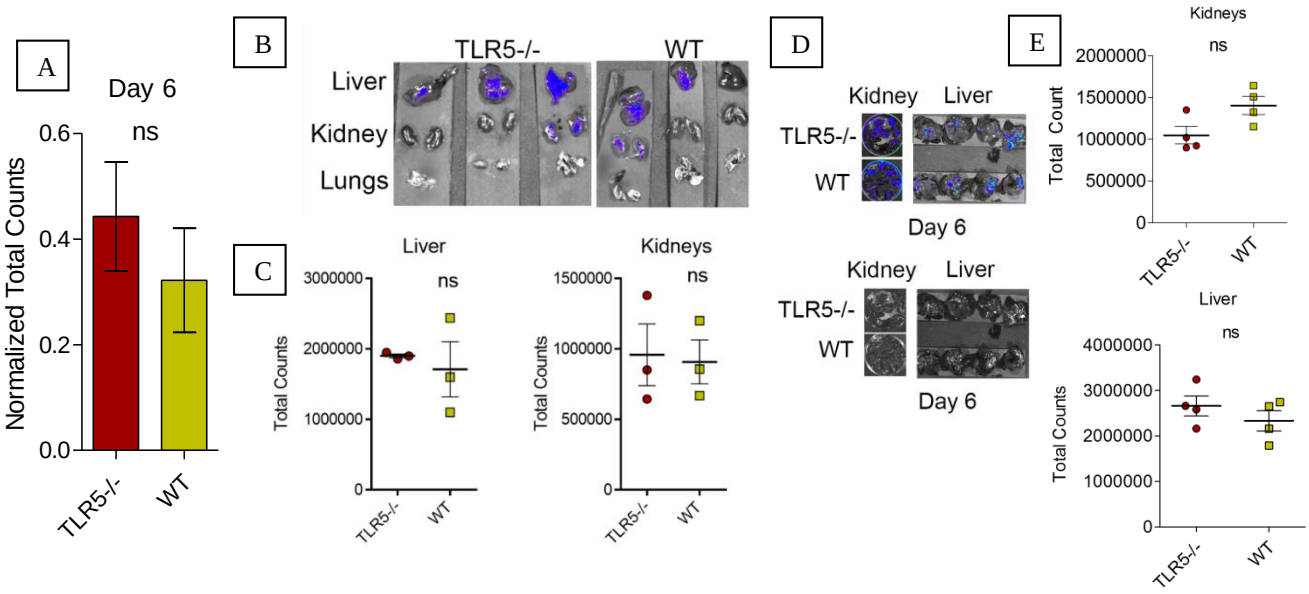

Fig. S4. PLGA nanoparticle trafficking from the injection site to lymphoid tissue on day 6 and accumulation in the liver and kidneys at days 2 and 6 after injection (related to Fig. 2). A) IVIS quantification demonstrating distribution of nanoparticles at Day 6 post injection for *TLR5-/-* and WT mice. Images are representative of a cohort of 4 mice. **B)** Fluorescent images showing accumulation of nanoparticle fluorescent signal in the liver and kidneys on day 2. **C**) Quantification of signal on day 2. (N=3) Statistical comparisons were performed by an unpaired, two tailed t-test. (ns denotes non-significant differences.) **D)** Fluorescent images showing accumulation of nanoparticle fluorescent signal in the liver and kidneys after day 6. **E**) Quantification of signal on day 6 from organs. (N=4) Statistical comparisons were performed by an unpaired, two tailed t-test. (ns denotes non-significant differences.)

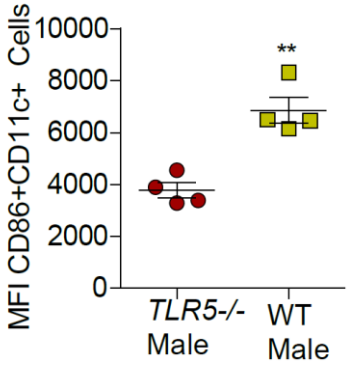

Fig. S5. Expression of CD86 activation marker (related to Fig. 2). *TLR5-/-* male mice express reduced levels of CD86 on the surface of CD86+CD11c+ antigen presenting cells when immunized with PLGA nanovaccines. (N=4) Statistical comparisons were performed by an unpaired, two tailed t-test. (** denotes $p < 0.001$)

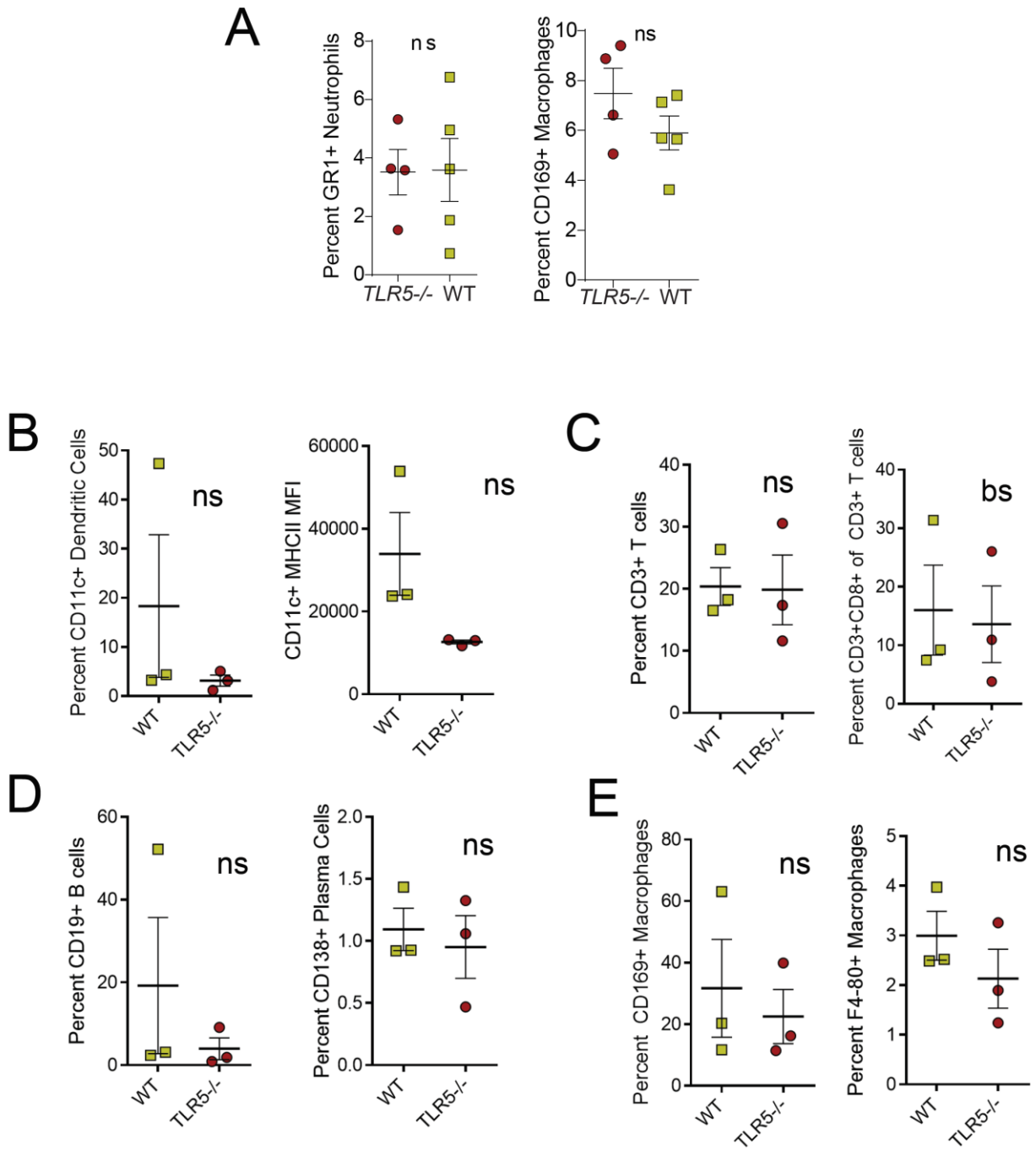

Fig. S6. Injection site analysis (related to Fig. 2). A) At the injection site on six days post injection, there were no differences in CD169+ macrophage or GR1+ neutrophil populations. Groups were compared using an unpaired, two tailed t-test. (N=4 *TLR5-/-*, N=5 WT) (ns denotes non-significant differences.) **(B-E)** On Day 2 post-injection, there are no differences lymphocytes in the injection site between *TLR5-/-* and WT mice. **B)** Left; Percent CD11c+ dendritic cells in the injection site. Right; MHCII median fluorescent intensity of dendritic cells in the injection site. **C**) Left; Percent CD3+ T cells in the injection site at Day 2. Right; Percent CD8+ T cells among CD3+ T cells. **D)** Left; Percent CD19+ B cells in the injection site. Right; Percent CD138+ Plasma cells in the injection site. **E)** Left; Percent C169+ macrophages in the injection site. Right; Percent F4-80+ macrophages in the injection site. All statistics were performed using an unpaired, two tailed t-test. (N=3) (ns denotes non-significant differences.)

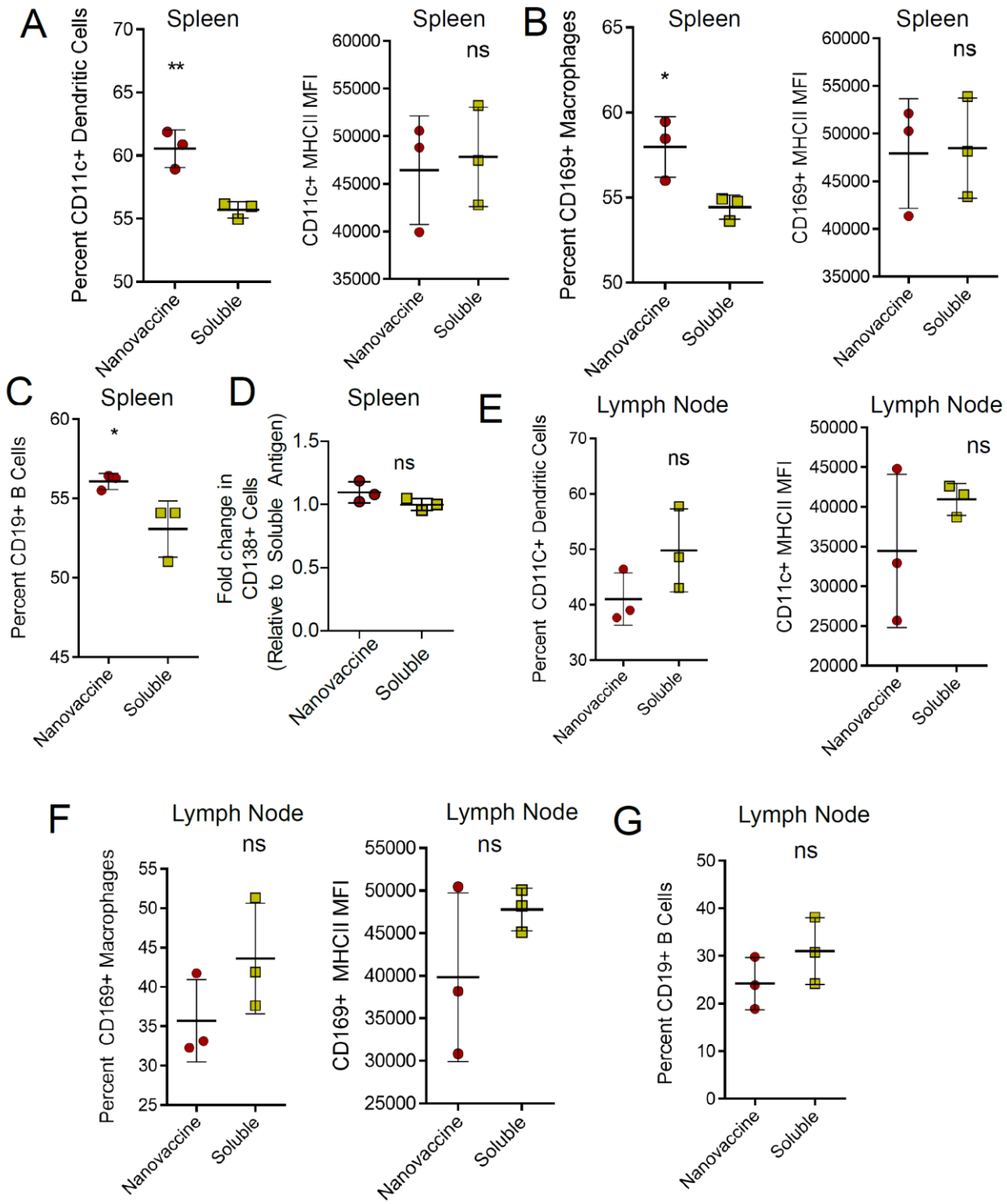

Fig. S7. Cell populations in the spleen and lymph node of immunized antibiotic-fed mice (related to Fig. 4). A) Left; percent CD11c+ dendritic cells. Right; MHCII MFI of CD11c+ dendritic cells. **B)** Left; percent CD169+ Macrophages.in the spleen. Right; MHCII MFI of these macrophages. **C)** Percent CD19+ B cells in the spleen. **D)** Fold change in CD138 cells relative to soluble. **E)** Left; percent CD11c+ dendritic cells in the lymph node. Right; MHCII MFI of these dendritic cells. **F)** Left; percent CD169+ macrophages in the lymph node. Right; MHCII MFI of these macrophages. **G)** Percent CD19+ B cells in the lymph node. All groups were compared with an unpaired, two tailed t test. (* denotes $p<0.05$, ** denotes $p<0.01$. ns denotes non-significant differences between groups.)

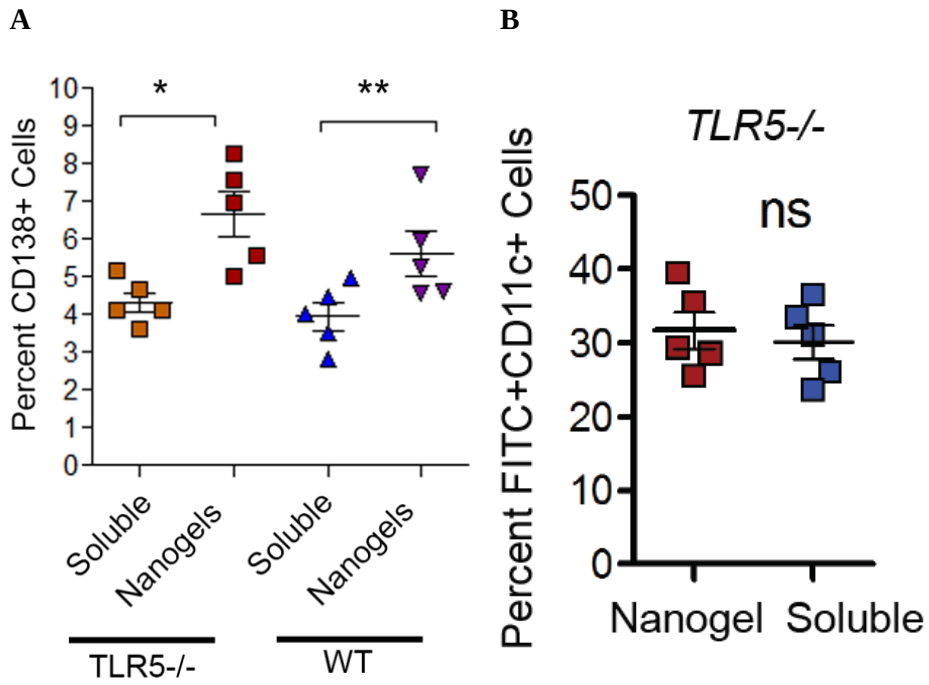

Fig. S8. Immunological characterization of Pyr-pHEMA nanogels (related to Fig. 5). (**A**) Pyr-pHEMA nanogels induce similar CD138+ immune response in WT and TLR5-/- mice. All nanogel groups were compared by an unpaired, two-tailed t-test with their soluble counterparts. In all the studies, *denotes $p<0.05$ and ***$p<0.001$. (**B**) **C**D11c+ dendritic cells in the lymphoid tissues of mice immunized with Pyr-pHEMA nanogel was compared to soluble. Comparisons were made by an unpaired, two-tailed t test, and all data is presented as Mean ± SEM. (N=5 Nanogel, N=5 Soluble formulation; ns denotes non-significant differences.).

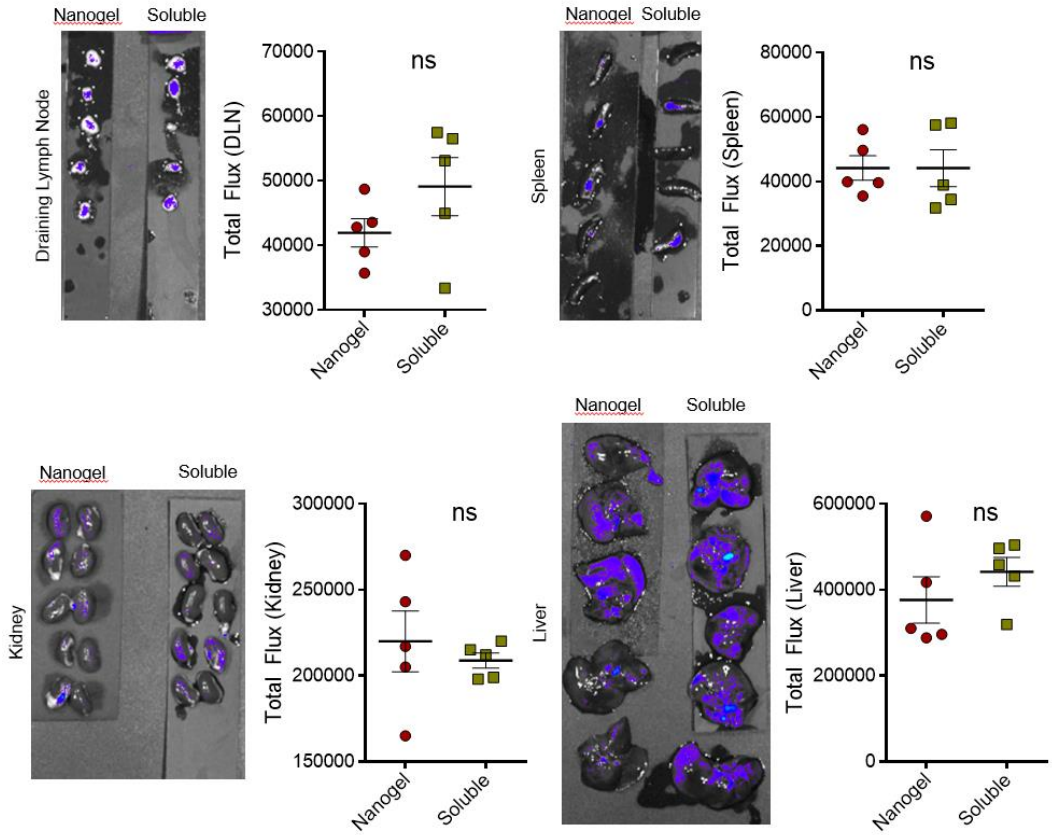

Fig. S9. Pyr-pHEMA nanogels do not differentially accumulate in tissue after 6 days relative to soluble formulation (related to Fig. 5). Fluorescent images of the draining lymph node, spleen, kidney, and liver six days after immunization. Scatter plot represent quantified total counts (flux) of IVIS signal. Groups were compared with an unpaired, two-tailed t-test. (ns denotes non-significant differences.)

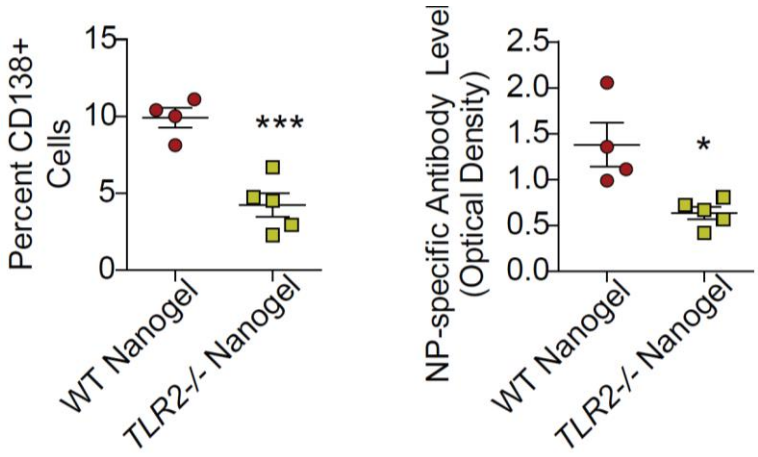

Fig. S10. Immunomodulatory effects of Pyr-pHEMA are mediated through TLR2 (related to Fig. 6). Percent CD138+ population between nanogel and soluble formulations (left) and NP-specific antibody levels (right). All nanogel groups were compared by an unpaired, two-tailed t-test with their soluble counterparts, and data is presented as Mean ± SEM. (N=4 WT Nanogel, N=5 *TLR2-/-* Nanogel). In all studies, *denotes $p<0.05$ and ***$p<0.001$.